Neuron
Review

Control of K_{Ca} Channels by Calcium Nano/Microdomains

Bernd Fakler[1,2,*] and John P. Adelman[3]
[1]Institute of Physiology, Engesser Str. 4, 79108 Freiburg, Germany
[2]Center for Biological Signaling Studies (bioss), Albert-Str. 19, 79104 Freiburg, Germany
[3]Vollum Institute, Oregon Health and Science University, Portland, Oregon 97239, USA
*Correspondence: bernd.fakler@physiologie.uni-freiburg.de
DOI 10.1016/j.neuron.2008.09.001

Transient elevations in cytoplasmic Ca^{2+} trigger a multitude of Ca^{2+}-dependent processes in CNS neurons and many other cell types. The specificity, speed, and reliability of these processes is achieved and ensured by tightly restricting Ca^{2+} signals to very local spatiotemporal domains, "Ca^{2+} nano- and microdomains," that are centered around Ca^{2+}-permeable channels. This arrangement requires that the Ca^{2+}-dependent effectors reside within these spatial boundaries where the properties of the Ca^{2+} domain and the Ca^{2+} sensor of the effector determine the channel-effector activity. We use Ca^{2+}-activated K^+ channels (K_{Ca}) with either micromolar (BK_{Ca} channels) or submicromolar (SK_{Ca} channels) affinity for Ca^{2+} ions to provide distance constraints for Ca^{2+}-effector coupling in local Ca^{2+} domains and review their significance for the cell physiology of K_{Ca} channels in the CNS. The results may serve as a model for other processes operated by local Ca^{2+} domains.

Introduction

In CNS neurons and many other cell types, intracellular calcium ions (Ca^{2+}) trigger a wide variety of Ca^{2+}-dependent signaling events and reaction cascades—sometimes with even opposing effects on cellular functions. To selectively orchestrate such a potentially complex range of Ca^{2+}-dependent reactions, the Ca^{2+} signal is precisely localized in time and space; the intracellular Ca^{2+} concentration ($[Ca^{2+}]_i$) is increased only for short periods of time and at spatially restricted domains. Such "local Ca^{2+} signaling domains" are generated by a variety of different Ca^{2+} buffer systems (mobile and immobile or fixed Ca^{2+}-binding systems) that limit the diffusion of Ca^{2+} ions after they have entered the cell through Ca^{2+}-permeable channels, mostly voltage-gated Ca^{2+} (Cav) channels (reviewed in detail by Augustine et al., 2003; Neher, 1998). In addition, the signaling systems that are fueled by Ca^{2+} are localized in close spatial proximity to the Ca^{2+}-permeable channels. This may be endowed either by direct physical association of the Ca^{2+} source and the Ca^{2+}-dependent target or by tethering the source and the target via specialized intermediary linkers or scaffolding proteins.

Experimentally, local Ca^{2+} signaling may be assessed by the Ca^{2+} chelators EGTA and BAPTA that compete for Ca^{2+} with the cellular Ca^{2+}-dependent targets. Both of these mobile Ca^{2+} buffers have similar steady-state binding affinities for Ca^{2+}; however, they largely differ in their binding rate constants, with BAPTA being about 150 times faster than EGTA (Naraghi and Neher, 1997). Accordingly, BAPTA is considerably more effective in preventing diffusion of free Ca^{2+} away from the entrance site at the plasma membrane; the concentration profile of free Ca^{2+} that is established at the cytoplasmic mouth of an open Ca^{2+}-permeable channel in the presence of BAPTA declines much more steeply with distance than the profile generated by equal concentrations of EGTA (see red and green lines in Figure 1; Matveev et al., 2004; Neher, 1986, 1998).

Based on these distinct characteristics, Neher (1998) and Augustine et al. (2003) proposed a BAPTA/EGTA-derived classification for local Ca^{2+} signaling domains: (1) processes that are effectively interfered with by BAPTA, but not EGTA, are placed in "Ca^{2+} nanodomains" (within ~20–50 nm of the Ca^{2+} source), while (2) processes that are equally sensitive to BAPTA and EGTA are located in "Ca^{2+} microdomains" (at distances between 50 nm and a few hundred nanometers from the Ca^{2+} source).

In either type of local Ca^{2+} domain, the magnitude and speed of the Ca^{2+} signal are inversely related to the distance between the Ca^{2+} source and the Ca^{2+} sensor, although on different scales. Thus, the peak $[Ca^{2+}]_i$ in nanodomains is about ten times higher than in microdomains (~100 μM versus 1–5 μM), and the rise and decay of the Ca^{2+} signal takes microseconds in Ca^{2+} nanodomains, while it occurs on the millisecond timescale in Ca^{2+} microdomains (Neher, 1986).

We will use examples from the two classes of Ca^{2+}-activated K^+ (K_{Ca}) channels that have distinct intrinsic affinities for Ca^{2+}, the voltage- and Ca^{2+}-activated large conductance K^+ (BK_{Ca}) channels and the Ca^{2+}-activated small conductance K^+ (SK_{Ca}) channels, as well as the recent results from proteomic and biochemical analyses of these two channel types to review the characteristics of channel gating by local Ca^{2+} signaling domains. We will survey distance constraints for coupling between K_{Ca} and Ca^{2+} sources for both BK_{Ca} and SK_{Ca} channels and discuss their relevance for the biology of these channels in the CNS.

Local Ca^{2+} Signaling and BK_{Ca} Channels

BK_{Ca} channels are involved in a diversity of physiological processes ranging from regulation of smooth muscle tone to modulation of neurotransmitter release (reviewed by Latorre and Brauchi, 2006; Sah and Faber, 2002; Vergara et al., 1998). In central neurons, where they are expressed throughout most regions of the mammalian brain (Sausbier et al., 2005), BK_{Ca} channels

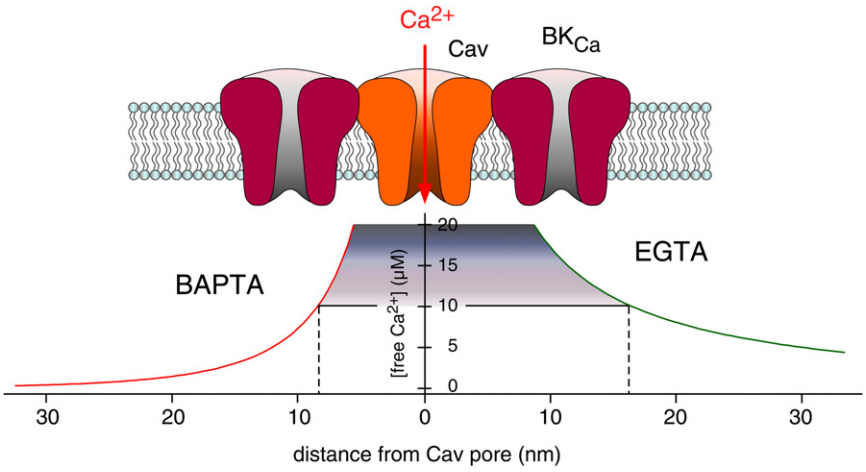

Figure 1. Prototypic Ca^{2+} Nanodomain: Bimolecular Complexes of BK_{Ca} and Cav Channels

Complex formation between BK_{Ca} and Cav channels guarantees $[Ca^{2+}]_i$ sufficiently high for reliable activation of BK_{Ca} at physiological voltages. BAPTA ($\geq$5 mM) interferes with functional coupling within the complex, while EGTA is ineffective (Berkefeld et al., 2006). The Ca^{2+} concentration profile at the cytoplasmic opening of the Cav subunit of the BK_{Ca}-Cav complex in the presence of 5 mM EGTA (green line) or 5 mM BAPTA (red line) was simulated with the CalC software v. 5.4.0 (Matveev et al., 2004); parameters used: Cav single-channel conductance of 1.7 pS, driving force for Ca^{2+} of 60 mV, channel opening of 1 ms, spherical geometry with a radius of 5 μm; binding constants and diffusion coefficients for both chelators were taken from Naraghi and Neher (1997). Dashed lines indicate the distance from the center of the Cav channel where the concentration of free Ca^{2+} drops below 10 μM, the threshold of $[Ca^{2+}]_i$ required for robust activation of BK_{Ca} in the physiological voltage range. For simplicity reasons, only one Cav channel was illustrated, although the subunit stoichiometry of BK_{Ca}-Cav complexes remains to be elucidated.

predominantly serve the following functions: they contribute to repolarization of the action potential (AP) (Storm, 1987a), mediate the fast phase of the afterhyperpolarization (fAHP) following an AP (Adams et al., 1982; Lancaster and Nicoll, 1987; Storm, 1987a), shape the dendritic Ca^{2+} spikes (Golding et al., 1999), and influence the release of neurotransmitters (Lingle et al., 1996; Petersen and Maruyama, 1984; Raffaelli et al., 2004; Robitaille et al., 1993). All of these CNS functions are fundamentally related to the unique gating of BK_{Ca} channels: they are activated by the cooperative effects of two distinct stimuli, membrane depolarization and cytoplasmic Ca^{2+}. Both stimuli converge allosterically on the gating apparatus of the channels, with increasing Ca^{2+} concentrations shifting the activation curve from highly positive potentials (>100 mV) into the physiological voltage range (Cui et al., 1997; Latorre et al., 1982; Marty, 1981). Robust activation of BK_{Ca} channels at membrane potentials around 0 mV requires values for $[Ca^{2+}]_i$ of $\geq$ 10 μM (Brenner et al., 2000), as are known to only occur in the immediate vicinity of active Ca^{2+} sources, particularly Cav channels. In most CNS neurons (and their subcellular compartments) where BK_{Ca} channel activation has been studied, the increase in $[Ca^{2+}]_i$ and membrane depolarization were coincidentally provided during the short duration of an AP. As we will discuss below, this imposes several spatial, temporal, and molecular constraints on the interaction between BK_{Ca} channels and their Ca^{2+} sources.

BK_{Ca} channels are tetramers of pore-forming BKα subunits that share the six-segment transmembrane (TM) topology of voltage-gated K^+ (Kv) channels, including the voltage-sensor domain (Adelman et al., 1992), but contain an additional TM domain at the N terminus (Meera et al., 1997). The cytoplasmic C terminus of BKα that comprises roughly two-thirds of the protein and is subjected to extensive pre-mRNA splicing and protein phosphorylation (Shipston, 2001; Yan et al., 2008) contains two regulating conductance of K^+ (RCK) domains and a string of aspartate residues known as the "Ca^{2+} bowl" (Schreiber and Salkoff, 1997). The tertiary folding of these domains is assumed to reconstitute a binding site for Ca^{2+} with micromolar affinities (K_d of 1–10 μM); binding of Ca^{2+} to this cytoplasmic site, in concert with depolarization, provides the energy required for opening of the channel pore in the membrane plane (Jiang et al., 2001, 2002; Xia et al., 2002; Yusifov et al., 2008). In addition, the gating properties of neuronal BK_{Ca} channels are influenced by auxiliary BKβ subunits (Knaus et al., 1994), two-TM domain proteins that modulate channel activation (time course and voltage dependence, BKβ2, 4) (Brenner et al., 2000; Uebele et al., 2000) and/or endow BK_{Ca} channels with a "ball-type" inactivation process (BKβ2) (Bentrop et al., 2001; Wallner et al., 1999; Xia et al., 1999).

BK_{Ca} Channels Form Macromolecular Complexes with Cav Channels and Establish a Prototypic Ca^{2+} Nanodomain

Investigations of BK_{Ca} channels in various types of neurons showed that the activation of BK_{Ca} channels requires the delivery of Ca^{2+} through Cav channels, as blocking these channels inhibits BK_{Ca}-mediated currents equally as well as removal of Ca^{2+} from the extracelluar milieu. In fact, Cav channel subtype-specific peptide toxins or reagents identified a set of Cav channels able to fuel BK_{Ca} channels: L-type (Prakriya and Lingle, 1999; Storm, 1987a), P/Q-type (Edgerton and Reinhart, 2003; Prakriya and Lingle, 1999; Womack et al., 2004), and N-type channels (Marrion and Tavalin, 1998). Additionally, the greater ability of BAPTA compared to EGTA to interfere with BK_{Ca} channel gating strongly suggested nanometer distances between the BK_{Ca} and Cav channels (Lancaster and Nicoll, 1987; Muller et al., 2007; Roberts, 1993; Storm, 1987b). The molecular mechanism linking the two types of channels has recently been resolved.

A proteomic approach that combined affinity purification with mass spectrometry showed that BK_{Ca} channels in the mammalian brain (composed of BKα and BKβ2/4) may exist in high-molecular weight complexes (~1.6 MDa) and identified several Cavα1 and Cavβ subunits that abundantly copurified with BKα-specific antibodies (Berkefeld et al., 2006). The Cavα1 subunits identified by mass spectrometric analyses were Cav1.2,

encoding the pore-forming subunit of L-type channels, and Cavs2.1 and 2.2, the molecular correlates of P/Q- and N-type channels (Catterall et al., 2005). Subsequent biochemical analyses of heterologously reconstituted BK_{Ca}-Cav complexes indicated that Cav and BK_{Ca} channels physically coassemble predominantly through their α subunits and that complex formation is Cav subtype specific, as Cav2.3, the correlate of R-type channels, failed to form stable macromolecular complexes with BK_{Ca} channels (Berkefeld et al., 2006).

When investigated in patch-clamp experiments, the heterologously expressed BK_{Ca}-Cav complexes displayed functional properties indistinguishable from those recorded from native cells under similar conditions (Berkefeld et al., 2006; Roberts, 1993). The current output of the complexes in response to step depolarizations was biphasic: an initial inward current carried by Ca^{2+} was followed by an outward K^+ current, reflecting the Cav channel that fuels the coassembled BK_{Ca} channel. Similar to neuronal cells, BK_{Ca}-Cav coupling occurred in the submillisecond range and was insensitive to EGTA even at concentrations as high as 10 mM (Berkefeld and Fakler, 2008; Berkefeld et al., 2006; Roberts, 1993; Yazejian et al., 2000). In contrast to the slow buffer EGTA, the K^+ current output of BK_{Ca}-Cav complexes was effectively diminished by millimolar concentrations of the fast chelator BAPTA ($\geq$5 mM) (Berkefeld et al., 2006), indicating that functional coupling in these channel-channel complexes obeyed the rules of Ca^{2+} nanodomains.

Figure 1 summarizes the molecular picture for assembly and functional properties of native and reconstituted BK_{Ca}-Cav complexes. Assuming a diameter for BK_{Ca} and Cav channels of ~10 nm, based upon the recently determined crystal structure of the Kv1.2 channel (Long et al., 2005), the cytoplasmic opening of the Cav channel and the Ca^{2+}-binding domain of the BK_{Ca} channel should be separated by at least this distance. In an EGTA-shaped Ca^{2+} concentration gradient, this distance ensures robust BK_{Ca} channel activity, equivalent to values for $[Ca^{2+}]_i$ of $\geq$ 10 μM (Berkefeld and Fakler, 2008; Berkefeld et al., 2006). In contrast, in a BAPTA-shaped concentration profile, activity of BK_{Ca} channels is reduced, indicating that $[Ca^{2+}]_i$ drops to values below the 10 μM threshold (Berkefeld et al., 2006). When these experimental results are compared with theoretical Ca^{2+} concentration gradients (based on Ca^{2+} influx, Ca^{2+}-binding kinetics, and diffusion of the chelator; red and green lines in Figure 1), there is reasonable agreement, as illustrated by the concentration-distance boundaries (dashed lines in Figure 1).

Thus, the macromolecular BK_{Ca}-Cav complexes that physically link a Ca^{2+} source and a Ca^{2+}-dependent effector may be regarded as prototypic Ca^{2+} nanodomains that provide experimentally verified criteria defining this type of local Ca^{2+} domain (see Introduction): (1) metric extension in the 10 nm range and (2) high BAPTA/EGTA efficacy for interference with the Ca^{2+}-mediated signaling.

Output of BK_{Ca}-Cav Complexes Is Tuned by the Distinct Cav Subunit

Formation of macromolecular complexes between BK_{Ca} and Cav channels (1) provides a simple mechanism for reliably delivering micromolar $[Ca^{2+}]_i$ to BK_{Ca} channels without affecting other Ca^{2+}-dependent signaling processes and (2) puts the activity of BK_{Ca} channels under tight control of the Cav partner. The impact of this Cav control over BK_{Ca} extends beyond reliable activation of BK_{Ca} channels and became evident from the K^+ current output of two distinct BK_{Ca}-Cav complexes, BK_{Ca}-Cav2.1 and BK_{Ca}-Cav1.2, reconstituted in heterologous expression systems. When stimulated with voltage pulses, BK_{Ca} channels (heteromers of BKα and BKβ4) coassembled with Cav2.1 channels activated markedly faster and at more negative membrane potentials than BK_{Ca} channels in complex with Cav1.2 channels, in line with the distinct gating properties of the two different Cav subtypes (Berkefeld and Fakler, 2008). Even more pronounced differences were observed with AP-like voltage commands of variable duration. While BK_{Ca}-Cav2.1 complexes provided robust K^+ currents even for APs with half-widths as short as 1 ms and over roughly two-thirds of the repolarization phase of the AP, BK_{Ca}-Cav1.2 complexes only responded to APs with half-widths longer than 1.8 ms and mediated K^+ currents for markedly shorter periods during the AP repolarization (Berkefeld and Fakler, 2008). According to these observations, the output characteristics of a particular BK_{Ca} channel are determined by the associated Cav subtype, offering a molecular mechanism to fine-tune the repolarizing K^+ current response and adapt BK_{Ca} channels to the requirement of particular neurons or subcompartments of neurons. In line with these results, BK_{Ca} channels were found to be predominantly fueled by P/Q-type Cav channels in cerebellar Purkinje cells with their narrow spikes and pronounced fAHPs (Edgerton and Reinhart, 2003; Womack et al., 2004), while in chromaffin cells, where APs typically last a few milliseconds, BK_{Ca} channels partner with both L-type and P/Q-type Cav channels (Berkefeld et al., 2006; Prakriya and Lingle, 1999).

BK_{Ca}-Cav Complexes and Uncomplexed BK_{Ca} Channels in CNS Neurons

There appears to be two classes of BK_{Ca} channels in neurons: those tightly associated with Cav channels in Ca^{2+} nanodomains and those located more distantly from Ca^{2+} sources. The latter population corresponds to Cav-free BK_{Ca} channels and reflects the fact that BK_{Ca} and Cav channels may be integrated into complexes (most likely in the endoplasmic reticulum) but may also be trafficked to the plasma membrane independently of each other.

While discussion of the range of examples is beyond the scope of this review, we will focus more on the two general categories of BK_{Ca} channels, as well as on reports that have elucidated both coupling to the Ca^{2+} source and the related physiology.

Nanodomain BK_{Ca}-Cav coupling as derived from high-capacity Ca^{2+} buffering was reported for BK_{Ca} channels and different Cav channel subtypes in several types of neuronal cells, including mammalian hippocampal pyramidal cells (L-type channels [Lancaster and Nicoll, 1987; Storm, 1987a, 1987b] and N-type channels [Marrion and Tavalin, 1998]), mammalian cerebellar Purkinje cells (P/Q-type channels [Edgerton and Reinhart, 2003; Womack et al., 2004]), frog hair cells (L- and N-type channels [Roberts, 1993, 1994; Roberts et al., 1990]), frog peripheral axonal terminals (N-type channels [Robitaille et al., 1993; Sun et al., 2004; Yazejian et al., 1997, 2000]), and mammalian chromaffin cells (P/Q- and L-type channels [Prakriya and Lingle, 1999; Prakriya et al., 1996; Solaro et al., 1995]). In these examples, BK_{Ca} channels are reliably activated by the short depolarization of an AP, similar to the results with reconstituted BK_{Ca}-Cav complexes (Berkefeld and Fakler, 2008), reinforcing the

idea that BK_{Ca} and Cav channels are coassembled. As a result of the AP-triggered depolarization and influx of Ca^{2+} through coupled Cav channels, BK_{Ca} channels provide a K^+ conductance that contributes to repolarization of the AP and gives rise to the fAHP of the membrane potential (Lancaster and Nicoll, 1987; Storm, 1987a, 1987b). The contribution to AP repolarization and generation of the fAHP are readily revealed upon blocking BK_{Ca} channels (with TEA, peptide toxins, or paxilline) that broadens the APs and selectively abolishes the fAHP, and, as a consequence, changes the neuronal firing pattern (Edgerton and Reinhart, 2003; Lancaster et al., 1991; Shao et al., 1999; Storm, 1987a). Interestingly, in CA1 neurons, the BK_{Ca}-mediated effects are apparent early in a train of APs, but, as the train progresses, BK_{Ca} channels successively inactivate, presumably induced by the coassembled BKβ2 subunit, when the frequency of AP-triggered channel activation exceeds the rate of recovery from inactivation. This reduces the number of available BK_{Ca} channels, similar to their block by exogenous agents (Shao et al., 1999), and results in AP broadening and reduction of the fAHP during a train of APs. In presynaptic terminals, the BK_{Ca}-mediated repolarization of the AP exerts an additional effect closely related to the role of $[Ca^{2+}]_i$ in triggering membrane fusion of synaptic vesicles and transmitter release. Presynaptic BK_{Ca} channels curtail the opening of Cav channels, thereby terminating the Ca^{2+} influx and, hence, the release of neurotransmitters by decreasing $[Ca^{2+}]_i$ below the threshold for vesicle fusion. This BK_{Ca}-based negative feedback mechanism contributes to precise timing of synaptic transmission and prevents overexcitation (Pattillo et al., 2001; Raffaelli et al., 2004; Robitaille et al., 1993).

Distinct from localization in Ca^{2+} nanodomains, BK_{Ca} channels may also be operated by more distant Ca^{2+} sources or by a global increase in $[Ca^{2+}]_i$. Thus, in chromaffin cells, BK_{Ca} channels were readily inhibited by submillimolar concentrations of EGTA (Prakriya and Lingle, 2000; Prakriya et al., 1996), and, in axon terminals of CA3 pyramidal cells, BK_{Ca} channels were only activated upon an increase in $[Ca^{2+}]_i$ markedly beyond that triggered by single APs (Hu et al., 2001). Although the physiological significance of these uncomplexed BK_{Ca} channels is not yet fully understood, a role as an "emergency brake" has been hypothesized, preventing cell damage or apoptosis under pathophysiological conditions that result in an extraordinarily large Ca^{2+} transient (Hu et al., 2001).

Ca^{2+} Signaling and SK_{Ca} Channels

SK_{Ca} are widely expressed in the CNS, where they are important for intrinsic excitability and pacemaking (Wolfart et al., 2001), dendritic integration (Cai et al., 2004), and shaping postsynaptic responses (Ngo-Anh et al., 2005), as well as modulating (Stackman et al., 2002) and contributing to synaptic plasticity (Lin et al., 2008). In different neuronal cell types and even within different subcellular compartments of the same neurons, SK_{Ca} channels may be gated by elevations of $[Ca^{2+}]_i$ mediated by different classes of Ca^{2+} sources, and, in this sense, they differ from the tight coupling between Cav and BK_{Ca} channels discussed above. In many but not all cases, SK_{Ca} channel activity feeds back to the Ca^{2+} source and limits Ca^{2+} influx, thereby shaping the amplitude and duration of the Ca^{2+} transient and influencing the many downstream signaling pathways that are affected by elevated cytoplasmic Ca^{2+} levels.

SK_{Ca} Channels Use Calmodulin as a High-Affinity Ca^{2+} Sensor

SK_{Ca} channels are gated solely by intracellular Ca^{2+} ions. Although they share the six-transmembrane serpentine topology of Kv channels (Kohler et al., 1996), SK_{Ca} channels lack voltage dependence to their open probability even at extreme membrane potentials, in contrast to their large conductance BK_{Ca} cousins (Hirschberg et al., 1998). All four members of the SK_{Ca} channel family share a conserved gating mechanism. SK_{Ca} channels are heteromeric complexes of the four SK_{Ca} pore-forming α subunits and calmodulin (CaM), with each α subunit harboring a constitutively bound CaM. When Ca^{2+} ions bind to the N lobe EF-hands of CaM, a conformational change is induced in the SK_{Ca} channel complex that opens the gate of the channel; deactivation reflects Ca^{2+} unbinding (Keen et al., 1999; Xia et al., 1998b). SK_{Ca} channel activity shows a steep dependence upon $[Ca^{2+}]_i$ with a Hill coefficient of ~4 and an EC_{50} of ~0.5 μM. The use of CaM as a Ca^{2+} sensor endows SK_{Ca} channels with an intrinsically higher affinity for Ca^{2+} than the BK_{Ca} channels. However, the SK_{Ca} channel opening that involves conformational changes communicated between CaM and the SK_{Ca} α subunits is slower than the opening of BK_{Ca} channels; when SK_{Ca} channels are rapidly exposed to saturating $[Ca^{2+}]_i$, the activation time constants are ~5 ms, while deactivation upon rapid return to Ca^{2+}-free solution occurs with time constants of ~30 ms (Pedarzani et al., 2001; Xia et al., 1998a).

SK_{Ca} Ca^{2+} Gating Is Modulated by Protein Phosphorylation

The Ca^{2+} sensitivity of SK_{Ca} channels is finely regulated by protein kinase CK2 and protein phosphatase 2A (PP2A) that, in addition to CaM, are also constitutively bound components of the SK_{Ca} channel complex (Allen et al., 2007; Bildl et al., 2004). SK_{Ca}-bound CK2 does not phosphorylate the channel α subunits. Rather, CK2 phosphorylates SK_{Ca}-bound CaM at position T80, reducing the apparent Ca^{2+} sensitivity of the channels and shifting the EC_{50} and Hill coefficient to ~2 μM and 2, respectively. Inhibiting CK2, which allows SK_{Ca}-bound PP2A to fully dephosphorylate SK_{Ca}-bound CaM, shifts the EC_{50} and Hill coefficient to ~0.3 μM and >4, respectively. The effects of CK2 and PP2A are reflected in the channel kinetics; when CK2 phosphorylates SK_{Ca}-bound CaM, the deactivation rates are ~4-fold faster than for the unphosphorylated channels (Allen et al., 2007; Bildl et al., 2004). Moreover, the ability of CK2 to phosphorylate SK_{Ca}-bound CaM is state dependent, occurring only when the channels are in the closed state (Allen et al., 2007). This state dependence adds an additional level of Ca^{2+} regulation to the SK_{Ca} channels; the Ca^{2+}-dependent gating apparatus becomes itself Ca^{2+} dependent and will be dynamically tuned as the local Ca^{2+} concentration changes. Indeed, during a Ca^{2+} transient, while the concentration of Ca^{2+} in the microenvironment of the SK_{Ca} channels is changing, the Ca^{2+} sensitivity of the channels will rapidly slide along the concentration gradient (Figure 3).

Recent results show that CK2/PP2A tuning of SK_{Ca} channels mediates neurotransmitter modulation of SK_{Ca} currents

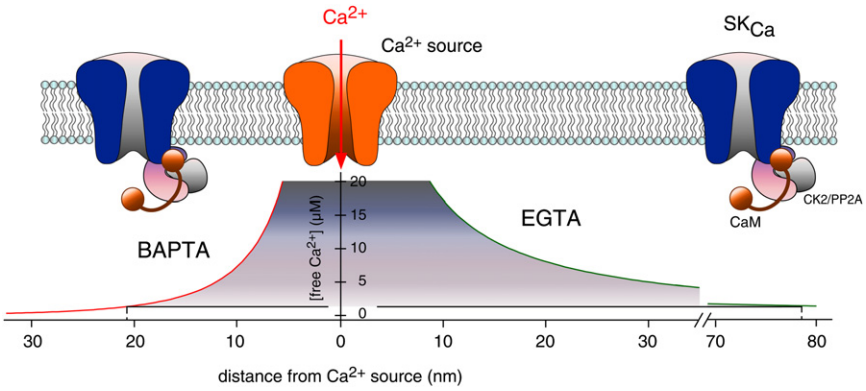

Figure 2. Ca^{2+} Nano- or Microdomain: Colocalization of SK_{Ca} and Ca^{2+}-Permeable Channels

Colocalization of Ca^{2+} source and SK_{Ca} channel complexes composed of SKα, CaM, protein kinase CK2, and protein phosphatase 2A. Ca^{2+} profiles are as in Figure 1. Dashed lines indicate the distance of the $[Ca^{2+}]_i$ threshold of 1 μM required for robust activation of SK_{Ca}. For simplicity reasons, only one Ca^{2+} source was illustrated.

(Maingret et al., 2008). In recordings from microvesicles prepared from sympathetic superior cervical ganglion neurons, single SK_{Ca} channel openings were fueled by Ca^{2+} influx through either endogenous N- or transfected R-type Cav channels. Noradrenaline application inhibited SK_{Ca} channels, apart from effects on the Cav channels, and inhibition was due to decreased Ca^{2+} sensitivity of the SK_{Ca} channels mediated by CK2 phosphorylation of SK_{Ca}-associated CaM. Similar regulation of SK_{Ca} channels was shown in small, dorsal root ganglion cells, putative nociceptors where norepinephrine application increased excitability, increasing the number of action potentials elicited by a given current injection.

Even the fully dephosphorylated form of the SK_{Ca} channels, with an EC_{50} ~0.3 μM, does not reflect the maximal Ca^{2+} sensitivity endowed to SK_{Ca} channels by the CaM Ca^{2+} sensor (Allen et al., 2007; Bildl et al., 2004). This is revealed by application of compounds such as 1-EBIO (1-ethyl-2-benzimidazolinone) or NS309 (6,7-dichloro-1H-indole-2,3-dione 3-oxime), which decrease the EC_{50} for Ca^{2+} by almost another order of magnitude to ~0.07 μM. These compounds are not true activators because they are ineffective in the absence of Ca^{2+}; rather, they act on the Ca^{2+} gating apparatus, primarily slowing the deactivation rate of the channels by stabilizing the Ca^{2+}-CaM-SK_{Ca} interaction (Pedarzani et al., 2001). The effects of the physiologically relevant CK2/PP2A and the drugs 1-EBIO and NS309 illustrate that SK_{Ca} channels are exquisitely poised to respond to physiological fluctuations of $[Ca^{2+}]_i$ and that the intrinsic apparent affinity of Ca^{2+} gating may be modulated.

SK_{Ca} channels are not directly coassembled with their Ca^{2+} sources (Figure 2). Unlike BK_{Ca} channels, where there may be a single coassembled Cav channel fueling a single BK_{Ca} channel, SK_{Ca} channels likely are contained within a microdomain with more than a single Ca^{2+} source providing the Ca^{2+} for SK_{Ca} channel activation. Due to their intrinsically higher Ca^{2+} sensitivity, SK_{Ca} channels may be located as far as several tens of nanometers away from the Ca^{2+} sources that are still capable of providing essentially saturating $[Ca^{2+}]_i$ at rates that are faster than the intrinsic activation kinetics of the SK_{Ca} channels (Figure 2). Similarly, the decay of the local Ca^{2+} transient occurs faster than the closing rate of the SK_{Ca} channels. Therefore, in many but not all cases, SK_{Ca} channel gating itself becomes rate limiting (Cueni et al., 2008; Marrion and Tavalin, 1998; Oliver et al., 2000).

SK_{Ca} Channels Are Coupled to Different Ca^{2+} Sources

L-type Cav Channels and SK_{Ca} Channels. The first study that demonstrated a direct, discrete coupling between a Ca^{2+} source and SK_{Ca} channel activity was from acutely dissociated CA1 hippocampal pyramidal neurons (Marrion and Tavalin, 1998). Using somatic, cell-attached patch recordings of single-channel activities, depolarizing commands elicited brief Ca^{2+} inward currents through L-type Cav channels that were frequently followed by outward-going K^+ currents mediated by SK_{Ca} channels. Both Cav and SK_{Ca} channel openings were abolished by nimodipine, suggesting that, in isolated CA1 neurons, somatic L-type channels supply the Ca^{2+} to activate SK_{Ca} channels. Moreover, the latency between Cav and SK_{Ca} channel openings was consistent with the activation time constant obtained for cloned SK2 channels at a $[Ca^{2+}]_i$ of 1 μM. These data confirm the spatial relation between Ca^{2+} source and SK_{Ca} channel illustrated in Figure 2. Based upon the EGTA/BAPTA-shaped Ca^{2+} concentration profiles and the known Ca^{2+} sensitivity of SK_{Ca} channels, a concentration of ~1 μM is expected at a distance of 20–100 nm from the internal mouth of the Cav channel (Figure 2), providing a metric for the distance separating the two channel types in acutely isolated CA1 neurons. This estimate was reinforced by the ability of the rapid, high-affinity Ca^{2+} buffer BAPTA to reduce the coupling between L-type Cav channels and SK_{Ca} channels (Marrion and Tavalin, 1998).

Acetylcholine Receptors and SK_{Ca} Channels. Auditory outer hair cells (OHCs) present a unique inhibitory synapse that uses excitatory Ca^{2+}-permeable nicotinic acetylcholine receptors (nAChRs), including the α9/α10 subunits, for fast inhibitory synaptic transmission (Elgoyhen et al., 2001; Oliver et al., 2001; Vetter et al., 1999); Ca^{2+} that enters the postsynaptic hair cell through nAChRs activates SK2 channels, which, in turn, provide a repolarizing and, hence, inhibitory K^+ conductance (Oliver et al., 2000; Yuhas and Fuchs, 1999). The activation and decay time course of the unitary IPSCs of this synapse are shaped by the activation/deactivation kinetics of SK2 channels (Bildl et al., 2004; Oliver et al., 2000). Thus, the kinetics of OHC IPSCs and K^+ currents recorded upon rapid application of 10 μM Ca^{2+} to heterologously expressed, low-affinity SK2-phospho-CaM channels in inside-out patches were virtually identical, and application of 1-EBIO increased the IPSC decay time constant to a similar extent as the deactivation of SK2 channels (Bildl et al., 2004; Oliver et al., 2000; Pedarzani et al., 2001; Xia et al.,

1998b). Finally, dialysis of OHCs with the fast Ca^{2+} buffer BAPTA (5 mM), but not EGTA (5 mM), reduced the amplitude of IPSCs without altering their kinetics (Oliver et al., 2000). Together, the properties of the nAChR-SK2 coupling show that, in OHCs, both types of channels are packaged into a Ca^{2+} nanodomain, with at least some channels residing within 15–20 nm of each other (Figure 2). Functionally, this spatial arrangement of a rapidly gating Ca^{2+} source and SK_{Ca} channels (onset/decay of nAChR currents faster than the activation/deactivation of SK2 channels) recapitulates an inhibitory synapse with transmission kinetics similar to those of the classical GABAergic or glycinergic synapses (Jonas et al., 1998; Jones and Westbrook, 1996; Takahashi and Momiyama, 1991).

NMDA Receptors, R-Type Ca^{2+} Channels, and SK_{Ca} Channels. In CA1 neurons, SK2 channels are expressed throughout the dendrites where they are fueled by Cav channels (Cai et al., 2004), while, in dendritic spines, SK2 channels are activated by synaptically evoked Ca^{2+} influx through NMDA-type glutamate receptors (NMDAr) and R-type Cav channels (Bloodgood and Sabatini, 2007; Ngo-Anh et al., 2005). The repolarizing influence of spine SK2 channels shunts the depolarization mediated by AMPA-type glutamate receptors. As a consequence, the EPSP is decreased, the voltage-dependent Mg^{2+} block of NMDAr is reinstated, and R-type Cav channels deactivate, which attenuates the spine Ca^{2+} transient (Bloodgood and Sabatini, 2007; Ngo-Anh et al., 2005). Whole-cell dialysis with BAPTA (5 mM), but not with the same concentration of EGTA, effectively turned down coupling between NMDAr and SK2 channels, suggesting that both reside in a nanodomain distance of ~20–50 nm (see Figure 2) within the confined Ca^{2+} signaling compartment of the dendritic spine (Ngo-Anh et al., 2005). This conclusion is supported by double label, postembedding immunogold electron microscopy that detected SK2 channels and NMDAr within the postsynaptic density (Lin et al., 2008).

T-Type Ca^{2+} Channels, SERCA, and SK_{Ca} Channels. In the thalamus, the nucleus reticularis (nRt) is a thin inhibitory network interposed between thalamocortical projection neurons and the cortex that is important for information transfer and arousal control. Low-threshold, T-type Cav currents underlie the rhythmic burst discharges during neuronal oscillations typical for sleep (Contreras, 2006; Crunelli et al., 2006). In the dendrites of nRt neurons, T-type Cav channels are heavily expressed, and Ca^{2+} influx through T-type channels is the predominant basis for dendritic Ca^{2+} transients. Immunogold EM showed that SK2 channels are also expressed in nRt dendrites, and, although depolarizing voltage commands evoke an apamin-sensitive current that is partially blocked by blocking P/Q- and N-type channels, the Ca^{2+} activating SK2 channels in dendrites is selectively supplied by T-type channels. The latency between the peak of the T-type current and the peak of the SK2 current is consistent with the activation kinetics of the SK2 channels. These results suggest that the T-type channels in nRt dendrites rapidly supply saturating $[Ca^{2+}]_i$ for SK2 channel activation, and blocking the SK2 current showed that the repolarizing SK2 channel activity feeds back to accelerate the deactivation of the T-type channels, consistent with the role of SK2 channels in promoting oscillations. The rapid activation of dendritic SK2 channels by Ca^{2+} entering through T-type channels suggests that they may be coassembled in a Ca^{2+} nanodomain. However, BAPTA and EGTA (5 mM) were equally effective at interrupting the Ca^{2+} coupling between the two channel types, suggesting that the SK2 channels and the T-type Ca^{2+} channels are more than 75 nm apart (see Figure 2). Therefore, the rapid coupling is due to a high density of T-type channels in the long, thin dendrites of nRt neurons that rapidly give rise to a large, relatively uniform increase in Ca^{2+} that obviates the need for nanodomain spatial proximity of the T-type Ca^{2+} source and the SK2 channel. In addition, in nRt dendrites, the SK2 current is attenuated by the endoplasmic Ca^{2+} pump, SERCA. Contrary to expectation, blocking SERCA activity enhanced and prolonged the SK2 current, and this was due to blocking the reuptake of Ca^{2+} into internal stores by SERCA (Cueni et al., 2008). Thus, in nRt neurons, SK2 channels and SERCA compete for Ca^{2+} ions that enter through T-type Ca channels and thereby shape the Ca^{2+} transient and oscillatory bursts.

K_{Ca} Channels and Endogenous Buffer Systems

The exogenous buffers BAPTA and EGTA, with their distinct Ca^{2+}-binding properties, are versatile tools for characterizing the coupling between Ca^{2+} source and target under standardized conditions and for estimating their spatial arrangement in local Ca^{2+} signaling domains. Physiological Ca^{2+} buffers, however, may behave differently and set up local Ca^{2+} domains with extensions different than those generated by the exogenous buffer systems. Several elegant reports have attempted to close this gap by comparing the buffer capacity of endogenous buffers to the capacity of EGTA/BAPTA in different cell types using BK_{Ca} channel activity or fluorescence-based Ca^{2+} imaging (Jackson and Redman, 2003; Muller et al., 2005, 2007; Roberts, 1993, 1994). Figure 3 illustrates respective Ca^{2+} profiles generated by endogenous buffer systems (such as calbindin or parvalbumin) with the minimal and maximal buffer capacity described for neuronal cell types together with the derived distance boundaries for reliable activation of K_{Ca} channels. Accordingly, the efficacy and range of reliable coupling between Ca^{2+} source and K_{Ca} are inversely related to the Ca^{2+} affinity of the respective channel; while the low-affinity BK_{Ca} channels (requiring $[Ca^{2+}]i \geq 10\ \mu M$) are robustly activated when located within 10–30 nm of the Ca^{2+} source, SK_{Ca} channels may reside within roughly 20–70 nm (low-affinity channels with phospho-CaM, requiring $[Ca^{2+}]i \geq 5\ \mu M$) or between 40 and >200 nm (high-affinity channels with dephospho-CaM, requiring $[Ca^{2+}]i \geq 1\ \mu M$) from the Ca^{2+} source. Similar spatial arrangements may be expected for the interaction between Ca^{2+} sources and Ca^{2+}-dependent targets with affinities for Ca^{2+} comparable to those of K_{Ca} channels.

Future Perspectives

The core molecular determinants of BK_{Ca} and SK_{Ca} channel signaling, including the pore-forming α subunits as well as a range of stably coassembled β subunits that modulate the effective Ca^{2+} sensitivity, alter channel kinetics, or both have been elucidated, and it is likely that more components of these macromolecular signaling complexes will be identified. Moreover, the spatiotemporal relationships between the BK_{Ca} and SK_{Ca} channels and their Ca^{2+} sources are becoming clear. It also seems very likely that, in addition to the stable interactions between K_{Ca} channels and coassembled modulatory proteins, important aspects of K_{Ca} signaling will be endowed by effectors that undergo

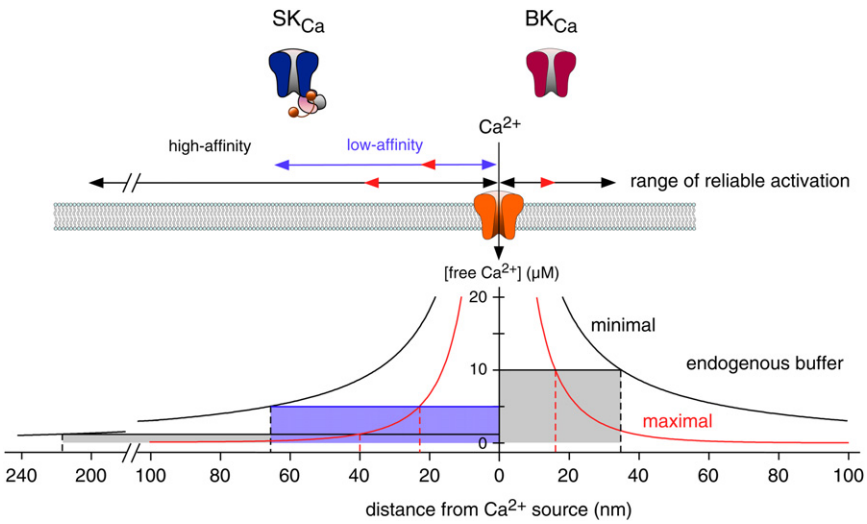

Figure 3. Spatial Constraints for the Coupling between K_{Ca} Channels and Ca^{2+} Sources under Physiological Buffer Conditions

Distance constraints for reliable activation of BK_{Ca} and SK_{Ca} channels under physiological conditions for Ca^{2+} buffering. Capacity/efficiency of the endogenous buffer was taken from Roberts (1993) (red line, annotated as "maximal" buffering, equivalent to 1.6 mM BAPTA) and from Müller et al. (2005) and Jackson/Redman (2003) (black line, annotated as "minimal" buffering, equivalent to ~100 μM EGTA) and simulated with the CalC software as in Figure 1. For SK_{Ca} channels, constraints were separated with respect to the high-affinity (CaM fully dephosphorylated, range of activation represented by the area shaded in gray) and low-affinity (CaM phosphorylated by CK2, range of activation represented by the area shaded in blue) states for Ca^{2+} binding. Again, only one Ca^{2+} source was depicted for simplicity reasons.

only transient, regulated forays into the K_{Ca} channel vicinity, within the signaling nano- or microdomains. Understanding these additional interactions and their consequences will provide insights into larger-scale Ca^{2+} signaling networks.

Precise regulation of the distance between Ca^{2+} sources and effectors, exemplified by the BK_{Ca} and SK_{Ca} models, is likely important for other fundamental processes in neurons and other cell types. For example, recent work shows that neurotransmitter release at the basket cell-granule cell synapse in the dentate gyrus, a process fueled by Ca^{2+} influx through P/Q-type Cav channels, is sensitive to BAPTA but insensitive to EGTA, suggesting a close nanodomain coupling between the Cav channels and the Ca^{2+} sensor for vesicle exocytosis (Bucurenciu et al., 2008). This is different than other cortical synapses (Borst and Sakmann, 1996; Ohana and Sakmann, 1998), and limiting the diffusional component of synaptic delay endows the basket cell-granule cell synapse with rapid signaling. These findings suggest that, by regulating the distance between the Ca^{2+} source and the Ca^{2+} sensor, synapses may tune their response kinetics (Rozov et al., 2001).

Ca^{2+} is the most widespread and diverse signaling messenger. Undoubtedly, as we develop new tools to more precisely study the dynamics of Ca^{2+} nano- and microdomains and their coupled activities, additional examples and variations will emerge that will illuminate the cellular and molecular mechanisms that coordinate Ca^{2+}-dependent processes.

ACKNOWLEDGMENTS

We thank H. Berkefeld for help with the concentration profiles and insightful discussions on local signaling domains and U. Schulte for his comments and critical reading of the work.

REFERENCES

Adams, P.R., Constanti, A., Brown, D.A., and Clark, R.B. (1982). Intracellular Ca^{2+} activates a fast voltage-sensitive K^+ current in vertebrate sympathetic neurones. Nature *296*, 746–749.

Adelman, J.P., Shen, K.Z., Kavanaugh, M.P., Warren, R.A., Wu, Y.N., Lagrutta, A., Bond, C.T., and North, R.A. (1992). Calcium-activated potassium channels expressed from cloned complementary DNAs. Neuron *9*, 209–216.

Allen, D., Fakler, B., Maylie, J., and Adelman, J.P. (2007). Organization and regulation of small conductance Ca^{2+}-activated K^+ channel multiprotein complexes. J. Neurosci. *27*, 2369–2376.

Augustine, G.J., Santamaria, F., and Tanaka, K. (2003). Local calcium signaling in neurons. Neuron *40*, 331–346.

Bentrop, D., Beyermann, M., Wissmann, R., and Fakler, B. (2001). NMR structure of the "ball-and-chain" domain of KCNMB2, the beta 2-subunit of large conductance Ca^{2+}- and voltage-activated potassium channels. J. Biol. Chem. *276*, 42116–42121.

Berkefeld, H., and Fakler, B. (2008). Repolarizing responses of BK_{Ca}-Cav complexes are distinctly shaped by their Cav subunits. J. Neurosci. *28*, 8238–8245.

Berkefeld, H., Sailer, C.A., Bildl, W., Rohde, V., Thumfart, J.O., Eble, S., Klugbauer, N., Reisinger, E., Bischofberger, J., Oliver, D., et al. (2006). BK_{Ca}-Cav channel complexes mediate rapid and localized Ca^{2+}-activated K^+ signaling. Science *314*, 615–620.

Bildl, W., Strassmaier, T., Thurm, H., Andersen, J., Eble, S., Oliver, D., Knipper, M., Mann, M., Schulte, U., Adelman, J.P., and Fakler, B. (2004). Protein kinase CK2 is coassembled with small conductance Ca^{2+}-activated K^+ channels and regulates channel gating. Neuron *43*, 847–858.

Bloodgood, B.L., and Sabatini, B.L. (2007). Nonlinear regulation of unitary synaptic signals by CaV(2.3) voltage-sensitive calcium channels located in dendritic spines. Neuron *53*, 249–260.

Borst, J.G., and Sakmann, B. (1996). Calcium influx and transmitter release in a fast CNS synapse. Nature *383*, 431–434.

Brenner, R., Jegla, T.J., Wickenden, A., Liu, Y., and Aldrich, R.W. (2000). Cloning and functional characterization of novel large conductance calcium-activated potassium channel beta subunits, hKCNMB3 and hKCNMB4. J. Biol. Chem. *275*, 6453–6461.

Bucurenciu, I., Kulik, A., Schwaller, B., Frotscher, M., and Jonas, P. (2008). Nanodomain coupling between Ca^{2+} channels and Ca^{2+} sensors promotes fast and efficient transmitter release at a cortical GABAergic synapse. Neuron *57*, 536–545.

Cai, X., Liang, C.W., Muralidharan, S., Kao, J.P., Tang, C.M., and Thompson, S.M. (2004). Unique roles of SK and Kv4.2 potassium channels in dendritic integration. Neuron *44*, 351–364.

Catterall, W.A., Perez-Reyes, E., Snutch, T.P., and Striessnig, J. (2005). International Union of Pharmacology. XLVIII. Nomenclature and structure-function relationships of voltage-gated calcium channels. Pharmacol. Rev. *57*, 411–425.

Contreras, D. (2006). The role of T-channels in the generation of thalamocortical rhythms. CNS Neurol. Disord. Drug Targets *5*, 571–585.

Crunelli, V., Cope, D.W., and Hughes, S.W. (2006). Thalamic T-type Ca^{2+} channels and NREM sleep. Cell Calcium *40*, 175–190.

Cueni, L., Canepari, M., Lujan, R., Emmenegger, Y., Watanabe, M., Bond, C.T., Franken, P., Adelman, J.P., and Luthi, A. (2008). T-type Ca^{2+} channels, SK2 channels and SERCAs gate sleep-related oscillations in thalamic dendrites. Nat. Neurosci. *11*, 683–692.

Cui, J., Cox, D.H., and Aldrich, R.W. (1997). Intrinsic voltage dependence and Ca^{2+} regulation of mslo large conductance Ca^{2+}-activated K^+ channels. J. Gen. Physiol. *109*, 647–673.

Edgerton, J.R., and Reinhart, P.H. (2003). Distinct contributions of small and large conductance Ca^{2+}-activated K^+ channels to rat Purkinje neuron function. J. Physiol. *548*, 53–69.

Elgoyhen, A.B., Vetter, D.E., Katz, E., Rothlin, C.V., Heinemann, S.F., and Boulter, J. (2001). alpha10: a determinant of nicotinic cholinergic receptor function in mammalian vestibular and cochlear mechanosensory hair cells. Proc. Natl. Acad. Sci. USA *98*, 3501–3506.

Golding, N.L., Jung, H.Y., Mickus, T., and Spruston, N. (1999). Dendritic calcium spike initiation and repolarization are controlled by distinct potassium channel subtypes in CA1 pyramidal neurons. J. Neurosci. *19*, 8789–8798.

Hirschberg, B., Maylie, J., Adelman, J.P., and Marrion, N.V. (1998). Gating of recombinant small-conductance Ca^{2+}-activated K^+ channels by calcium. J. Gen. Physiol. *111*, 565–581.

Hu, H., Shao, L.R., Chavoshy, S., Gu, N., Trieb, M., Behrens, R., Laake, P., Pongs, O., Knaus, H.G., Ottersen, O.P., and Storm, J.F. (2001). Presynaptic Ca^{2+}-activated K^+ channels in glutamatergic hippocampal terminals and their role in spike repolarization and regulation of transmitter release. J. Neurosci. *21*, 9585–9597.

Jackson, M.B., and Redman, S.J. (2003). Calcium dynamics, buffering, and buffer saturation in the boutons of dentate granule-cell axons in the hilus. J. Neurosci. *23*, 1612–1621.

Jiang, Y., Pico, A., Cadene, M., Chait, B.T., and MacKinnon, R. (2001). Structure of the RCK domain from the E. coli K^+ channel and demonstration of its presence in the human BK channel. Neuron *29*, 593–601.

Jiang, Y., Lee, A., Chen, J., Cadene, M., Chait, B.T., and MacKinnon, R. (2002). Crystal structure and mechanism of a calcium-gated potassium channel. Nature *417*, 515–522.

Jonas, P., Bischofberger, J., and Sandkuhler, J. (1998). Corelease of two fast neurotransmitters at a central synapse. Science *281*, 419–424.

Jones, M.V., and Westbrook, G.L. (1996). The impact of receptor desensitization on fast synaptic transmission. Trends Neurosci. *19*, 96–101.

Keen, J.E., Khawaled, R., Farrens, D.L., Neelands, T., Rivard, A., Bond, C.T., Janowsky, A., Fakler, B., Adelman, J.P., and Maylie, J. (1999). Domains responsible for constitutive and Ca^{2+}-dependent interactions between calmodulin and small conductance Ca^{2+}-activated potassium channels. J. Neurosci. *19*, 8830–8838.

Knaus, H.G., Folander, K., Garcia-Calvo, M., Garcia, M.L., Kaczorowski, G.J., Smith, M., and Swanson, R. (1994). Primary sequence and immunological characterization of beta-subunit of high conductance Ca^{2+}-activated K^+ channel from smooth muscle. J. Biol. Chem. *269*, 17274–17278.

Kohler, M., Hirschberg, B., Bond, C.T., Kinzie, J.M., Marrion, N.V., Maylie, J., and Adelman, J.P. (1996). Small-conductance, calcium-activated potassium channels from mammalian brain. Science *273*, 1709–1714.

Lancaster, B., and Nicoll, R.A. (1987). Properties of two calcium-activated hyperpolarizations in rat hippocampal neurones. J. Physiol. *389*, 187–203.

Lancaster, B., Nicoll, R.A., and Perkel, D.J. (1991). Calcium activates two types of potassium channels in rat hippocampal neurons in culture. J. Neurosci. *11*, 23–30.

Latorre, R., and Brauchi, S. (2006). Large conductance Ca^{2+}-activated K^+ (BK) channel: activation by Ca^{2+} and voltage. Biol. Res. *39*, 385–401.

Latorre, R., Vergara, C., and Hidalgo, C. (1982). Reconstitution in planar lipid bilayers of a Ca^{2+}-dependent K^+ channel from transverse tubule membranes isolated from rabbit skeletal muscle. Proc. Natl. Acad. Sci. USA *79*, 805–809.

Lin, M.T., Lujan, R., Watanabe, M., Adelman, J.P., and Maylie, J. (2008). SK2 channel plasticity contributes to LTP at Schaffer collateral-CA1 synapses. Nat. Neurosci. *11*, 170–177.

Lingle, C.J., Solaro, C.R., Prakriya, M., and Ding, J.P. (1996). Calcium-activated potassium channels in adrenal chromaffin cells. Ion Channels *4*, 261–301.

Long, S.B., Campbell, E.B., and Mackinnon, R. (2005). Crystal structure of a mammalian voltage-dependent Shaker family K^+ channel. Science *309*, 897–903.

Maingret, F., Coste, B., Hao, J., Giamarchi, A., Allen, D., Crest, M., Litchfield, D.W., Adelman, J.P., and Delmas, P. (2008). Neurotransmitter modulation of small-conductance Ca^{2+}-activated K^+ channels by regulation of Ca^{2+} gating. Neuron *59*, 439–449.

Marrion, N.V., and Tavalin, S.J. (1998). Selective activation of Ca^{2+}-activated K^+ channels by co-localized Ca^{2+} channels in hippocampal neurons. Nature *395*, 900–905.

Marty, A. (1981). Ca-dependent K channels with large unitary conductance in chromaffin cell membranes. Nature *291*, 497–500.

Matveev, V., Zucker, R.S., and Sherman, A. (2004). Facilitation through buffer saturation: constraints on endogenous buffering properties. Biophys. J. *86*, 2691–2709.

Meera, P., Wallner, M., Song, M., and Toro, L. (1997). Large conductance voltage- and calcium-dependent K^+ channel, a distinct member of voltage-dependent ion channels with seven N-terminal transmembrane segments (S0–S6), an extracellular N terminus, and an intracellular (S9–S10) C terminus. Proc. Natl. Acad. Sci. USA *94*, 14066–14071.

Muller, A., Kukley, M., Stausberg, P., Beck, H., Muller, W., and Dietrich, D. (2005). Endogenous Ca^{2+} buffer concentration and Ca^{2+} microdomains in hippocampal neurons. J. Neurosci. *25*, 558–565.

Muller, A., Kukley, M., Uebachs, M., Beck, H., and Dietrich, D. (2007). Nanodomains of single Ca^{2+} channels contribute to action potential repolarization in cortical neurons. J. Neurosci. *27*, 483–495.

Naraghi, M., and Neher, E. (1997). Linearized buffered Ca^{2+} diffusion in microdomains and its implications for calculation of $[Ca^{2+}]$ at the mouth of a calcium channel. J. Neurosci. *17*, 6961–6973.

Neher, E. (1986). Concentration profiles of intracellular calcium in the presence of a diffusible chelator (Berlin: Springer-Verlag).

Neher, E. (1998). Vesicle pools and Ca^{2+} microdomains: new tools for understanding their roles in neurotransmitter release. Neuron *20*, 389–399.

Ngo-Anh, T.J., Bloodgood, B.L., Lin, M., Sabatini, B.L., Maylie, J., and Adelman, J.P. (2005). SK channels and NMDA receptors form a Ca^{2+}-mediated feedback loop in dendritic spines. Nat. Neurosci. *8*, 642–649.

Ohana, O., and Sakmann, B. (1998). Transmitter release modulation in nerve terminals of rat neocortical pyramidal cells by intracellular calcium buffers. J. Physiol. *513*, 135–148.

Oliver, D., Klocker, N., Schuck, J., Baukrowitz, T., Ruppersberg, J.P., and Fakler, B. (2000). Gating of Ca^{2+}-activated K^+ channels controls fast inhibitory synaptic transmission at auditory outer hair cells. Neuron *26*, 595–601.

Oliver, D., Ludwig, J., Reisinger, E., Zoellner, W., Ruppersberg, J.P., and Fakler, B. (2001). Memantine inhibits efferent cholinergic transmission in the cochlea by blocking nicotinic acetylcholine receptors of outer hair cells. Mol. Pharmacol. *60*, 183–189.

Pattillo, J.M., Yazejian, B., DiGregorio, D.A., Vergara, J.L., Grinnell, A.D., and Meriney, S.D. (2001). Contribution of presynaptic calcium-activated potassium currents to transmitter release regulation in cultured Xenopus nerve-muscle synapses. Neuroscience *102*, 229–240.

Pedarzani, P., Mosbacher, J., Rivard, A., Cingolani, L.A., Oliver, D., Stocker, M., Adelman, J.P., and Fakler, B. (2001). Control of electrical activity in central neurons by modulating the gating of small conductance Ca^{2+}-activated K^+ channels. J. Biol. Chem. *276*, 9762–9769.

Petersen, O.H., and Maruyama, Y. (1984). Calcium-activated potassium channels and their role in secretion. Nature *307*, 693–696.

Prakriya, M., and Lingle, C.J. (1999). BK channel activation by brief depolarizations requires Ca^{2+} influx through L- and Q-type Ca^{2+} channels in rat chromaffin cells. J. Neurophysiol. *81*, 2267–2278.

Prakriya, M., and Lingle, C.J. (2000). Activation of BK channels in rat chromaffin cells requires summation of Ca^{2+} influx from multiple Ca^{2+} channels. J. Neurophysiol. *84*, 1123–1135.

Prakriya, M., Solaro, C.R., and Lingle, C.J. (1996). $[Ca^{2+}]_i$ elevations detected by BK channels during Ca^{2+} influx and muscarine-mediated release of Ca^{2+} from intracellular stores in rat chromaffin cells. J. Neurosci. *16*, 4344–4359.

Raffaelli, G., Saviane, C., Mohajerani, M.H., Pedarzani, P., and Cherubini, E. (2004). BK potassium channels control transmitter release at CA3–CA3 synapses in the rat hippocampus. J. Physiol. *557*, 147–157.

Roberts, W.M. (1993). Spatial calcium buffering in saccular hair cells. Nature *363*, 74–76.

Roberts, W.M. (1994). Localization of calcium signals by a mobile calcium buffer in frog saccular hair cells. J. Neurosci. *14*, 3246–3262.

Roberts, W.M., Jacobs, R.A., and Hudspeth, A.J. (1990). Colocalization of ion channels involved in frequency selectivity and synaptic transmission at presynaptic active zones of hair cells. J. Neurosci. *10*, 3664–3684.

Robitaille, R., Garcia, M.L., Kaczorowski, G.J., and Charlton, M.P. (1993). Functional colocalization of calcium and calcium-gated potassium channels in control of transmitter release. Neuron *11*, 645–655.

Rozov, A., Burnashev, N., Sakmann, B., and Neher, E. (2001). Transmitter release modulation by intracellular Ca^{2+} buffers in facilitating and depressing nerve terminals of pyramidal cells in layer 2/3 of the rat neocortex indicates a target cell-specific difference in presynaptic calcium dynamics. J. Physiol. *531*, 807–826.

Sah, P., and Faber, E.S. (2002). Channels underlying neuronal calcium-activated potassium currents. Prog. Neurobiol. *66*, 345–353.

Sausbier, U., Sausbier, M., Sailer, C.A., Arntz, C., Knaus, H.G., Neuhuber, W., and Ruth, P. (2005). Ca^{2+}-activated K^+ channels of the BK-type in the mouse brain. Histochem. Cell Biol. *125*, 725–741.

Schreiber, M., and Salkoff, L. (1997). A novel calcium-sensing domain in the BK channel. Biophys. J. *73*, 1355–1363.

Shao, L.R., Halvorsrud, R., Borg-Graham, L., and Storm, J.F. (1999). The role of BK-type Ca^{2+}-dependent K^+ channels in spike broadening during repetitive firing in rat hippocampal pyramidal cells. J. Physiol. *521*, 135–146.

Shipston, M.J. (2001). Alternative splicing of potassium channels: a dynamic switch of cellular excitability. Trends Cell Biol. *11*, 353–358.

Solaro, C.R., Prakriya, M., Ding, J.P., and Lingle, C.J. (1995). Inactivating and noninactivating Ca^{2+}- and voltage-dependent K^+ current in rat adrenal chromaffin cells. J. Neurosci. *15*, 6110–6123.

Stackman, R.W., Hammond, R.S., Linardatos, E., Gerlach, A., Maylie, J., Adelman, J.P., and Tzounopoulos, T. (2002). Small conductance Ca^{2+}-activated K^+ channels modulate synaptic plasticity and memory encoding. J. Neurosci. *22*, 10163–10171.

Storm, J.F. (1987a). Action potential repolarization and a fast after-hyperpolarization in rat hippocampal pyramidal cells. J. Physiol. *385*, 733–759.

Storm, J.F. (1987b). Intracellular injection of a Ca^{2+} chelator inhibits spike repolarization in hippocampal neurons. Brain Res. *435*, 387–392.

Sun, X.P., Yazejian, B., and Grinnell, A.D. (2004). Electrophysiological properties of BK channels in Xenopus motor nerve terminals. J. Physiol. *557*, 207–228.

Takahashi, T., and Momiyama, A. (1991). Single-channel currents underlying glycinergic inhibitory postsynaptic responses in spinal neurons. Neuron *7*, 965–969.

Uebele, V.N., Lagrutta, A., Wade, T., Figueroa, D.J., Liu, Y., McKenna, E., Austin, C.P., Bennett, P.B., and Swanson, R. (2000). Cloning and functional expression of two families of beta-subunits of the large conductance calcium-activated K^+ channel. J. Biol. Chem. *275*, 23211–23218.

Vergara, C., Latorre, R., Marrion, N.V., and Adelman, J.P. (1998). Calcium-activated potassium channels. Curr. Opin. Neurobiol. *8*, 321–329.

Vetter, D.E., Liberman, M.C., Mann, J., Barhanin, J., Boulter, J., Brown, M.C., Saffiote-Kolman, J., Heinemann, S.F., and Elgoyhen, A.B. (1999). Role of alpha9 nicotinic ACh receptor subunits in the development and function of cochlear efferent innervation. Neuron *23*, 93–103.

Wallner, M., Meera, P., and Toro, L. (1999). Molecular basis of fast inactivation in voltage and Ca^{2+}-activated K^+ channels: a transmembrane beta-subunit homolog. Proc. Natl. Acad. Sci. USA *96*, 4137–4142.

Wolfart, J., Neuhoff, H., Franz, O., and Roeper, J. (2001). Differential expression of the small-conductance, calcium-activated potassium channel SK3 is critical for pacemaker control in dopaminergic midbrain neurons. J. Neurosci. *21*, 3443–3456.

Womack, M.D., Chevez, C., and Khodakhah, K. (2004). Calcium-activated potassium channels are selectively coupled to P/Q-type calcium channels in cerebellar Purkinje neurons. J. Neurosci. *24*, 8818–8822.

Xia, X., Hirschberg, B., Smolik, S., Forte, M., and Adelman, J.P. (1998a). dSLo interacting protein 1, a novel protein that interacts with large-conductance calcium-activated potassium channels. J. Neurosci. *18*, 2360–2369.

Xia, X.M., Fakler, B., Rivard, A., Wayman, G., Johnson-Pais, T., Keen, J.E., Ishii, T., Hirschberg, B., Bond, C.T., Lutsenko, S., et al. (1998b). Mechanism of calcium gating in small-conductance calcium-activated potassium channels. Nature *395*, 503–507.

Xia, X.M., Ding, J.P., and Lingle, C.J. (1999). Molecular basis for the inactivation of Ca^{2+}- and voltage-dependent BK channels in adrenal chromaffin cells and rat insulinoma tumor cells. J. Neurosci. *19*, 5255–5264.

Xia, X.M., Zeng, X., and Lingle, C.J. (2002). Multiple regulatory sites in large-conductance calcium-activated potassium channels. Nature *418*, 880–884.

Yan, J., Olsen, J.V., Park, K.S., Li, W., Bildl, W., Schulte, U., Aldrich, R.W., Fakler, B., and Trimmer, J.S. (2008). Profiling the phospho-status of the BK_{Ca} channel α subunit in rat brain reveals unexpected patterns and complexity. Mol. Cell. Proteomics, in press. Published online June 23, 2008. 10.1074/mcp.M800063-MCP200.

Yazejian, B., DiGregorio, D.A., Vergara, J.L., Poage, R.E., Meriney, S.D., and Grinnell, A.D. (1997). Direct measurements of presynaptic calcium and calcium-activated potassium currents regulating neurotransmitter release at cultured Xenopus nerve-muscle synapses. J. Neurosci. *17*, 2990–3001.

Yazejian, B., Sun, X.P., and Grinnell, A.D. (2000). Tracking presynaptic Ca^{2+} dynamics during neurotransmitter release with Ca^{2+}-activated K^+ channels. Nat. Neurosci. *3*, 566–571.

Yuhas, W.A., and Fuchs, P.A. (1999). Apamin-sensitive, small-conductance, calcium-activated potassium channels mediate cholinergic inhibition of chick auditory hair cells. J. Comp. Physiol. [A] *185*, 455–462.

Yusifov, T., Savalli, N., Gandhi, C.S., Ottolia, M., and Olcese, R. (2008). The RCK2 domain of the human BKCa channel is a calcium sensor. Proc. Natl. Acad. Sci. USA *105*, 376–381.